MANSOURA JOURNAL OF CHEMISTRY
Official Journal of Faculty of Science, Mansoura University, Egypt
E-mail: scimag@mans.edu.eg ISSN: 2974-4938

Synthesis, Characterization and Antimicrobial Potency of Novel Zinc(II) Complex Derived from Carbohydrazone Ligand

Mohab A. El-helw, Usama El-Ayaan, Gaber M. Abu El-Reash*

Chemistry Department, Faculty of Science, Mansoura University, ET-35516-Mansoura, Egypt

**** Correspondence to:*** *gaelreash@mans.edu.eg, 01000373155*

Received:11/1/2025
Accepted: 19/2/2025

Abstract: A novel carbohydrazone Schiff base chelate, $[Zn(L)(Cl)(H_2O)].Cl$, was successfully synthesized and its structural features were comprehensively characterized through elemental analysis (CHN), FT-IR, UV-visible spectroscopy, and conductance measurements. In addition, computational studies were carried out using material studio 2017. The optimized geometry and frontier molecular orbitals of the isolated complex were computed. Finally, the antimicrobial efficacy of the isolated complex were evaluated. The zinc complex showed potency against most tested strians, except for *Listeria* and *Aspergillus*.

keywords: carbohydrazone, antimicrobial, theortical studies, spectroscopic techniques.

1. Introduction

Schiff bases have been extensively studied because of their enhanced sensitivity and selectivity towards metal ions, as well as their structural resemblance to naturally occurring biological compounds [1, 2]. As a result, Schiff bases have garnered significant attention in the field of bioinorganic chemistry due to the increasing demand for pharmaceutical applications. Both Schiff bases and their metal complexes have demonstrated remarkable biological efficacy, particularly as antibacterial and anticancer agents [3-6]. Hydrazone compounds, featuring an azomethine (C=N) group conjugated with the lone electron pair of the nitrogen functional group are regarded as physiologically vital compounds, likely due to their capacity to form stable chelates with metals present within cellular environments [7]. From this perspective, the antimicrobial activity of carbohydrazide complexes has been evaluated against *B. subtilis*, *E. coli*, *S. aureus*, and *C. oxosporum* bacteria, as well as *C. albicans* fungi, demonstrating more promising results compared to the ligand alone [8-11]. Additionally, derivatives of aminoacetophenone have exhibited significant biological activity against *Staphylococcus aureus*, *Escherichia coli*, and *Bacillus subtilis* [12, 13], this can be attributed to the amino group's electron-donating ability [14]. In this study we aim to synthesis a novel Zn(II) complex derived from the reaction of carbohydrazide with 4-aminoacetophenone to form carbohydrazone Schiff base ligand and investigate its biological potency.

2. Experimental

2.1. Materials and Reagents

4-aminoacetophenone, carbohydrazide, DMSO, absolute ethanol, KCl, $ZnCl_2$ were obtained from suppliers such as Merck, Sigma-Aldrich, and BDH, and were utilized in their original state without further treatment.

2.2 Characterization

carbon, hydrogen, and nitrogen elemental analyses were performed using a Perkin-Elmer 2400 Series II analyzer, while the zinc(II) concentration was determined through a volumetric method [15].

Infrared spectra were measured using KBr discs in the range of 4000–400 cm^{-1} with a Mattson 5000 FTIR spectrophotometer. Additionally, UV-Vis. spectra were recorded at room temperature in DMSO using a UV2 Unicam spectrophotometer.

The molar conductance of the synthesized complex at a concentration of 1×10^{-3}M was measured using a conductivity meter, with

DMSO serving as the solvent at room temperature.

2.3. Synthesis of HL Ligand and Zn(II) Complex

As mentioned in our early work [16] HL ligand was synthesized by refluxing 1 mmol of carbohydrazide with 4-aminoacetophenone in 20 mL ethanol for 3 hours at 90°C. TLC was employed to determine the progress of the reaction, the obtained paige solid was filtered and washed using hot ethanolic solution and dried using calcium chloride desiccator. %yield = 75, mp (195–198) °C. Elemental analyses showed C (measured = 62.49%, calculated = 62.95%), H (measured = 5.98%, calculated = 6.21%), and N (measured = 25.98%, calculated = 25.91%).

In addition, Zn(II) complex was obtained by refluxing 1 mmol of $ZnCl_2$ metal salt with 1 mmol of HL ligand in ethanolic solution for 5 hours at 70 °C. TLC was employed to determine the progress of the reaction, the obtained yellow solid was filtered and washed using hot ethanolic solution and dried using calcium chloride desiccator. %yield = 69, mp (259) °C. Elemental analyses showed C (measured = 42.75%, calculated = 42.17%), H (measured = 4.43%, calculated = 4.89%), and N (measured = 17.59%, calculated = 18.09%), Zn(II) (measured =13.69%, calculated = 13.42%), Cl (measured = 14.84%, calculated = 14.55%).

Table (1): The analytical and physical data of $[Zn(L)(Cl)(H_2O)].Cl$ complex.

Complex (empirical formula)	Mwt (g mol^{-1})	Color	%measured(%calc)				
			C	H	N	M	Cl
$C_{17}H_{21}Cl_2ZnN_6O_2$	442.23	Yellow	42.75 (42.17)	4.43 (4.89	17.59 (18.09	13.69 (13.42	14.84 (14.55

2.4. Antimicrobial activities

The *in vitro* antimicrobial screening of the isolated HL ligand and its Zn(II) novel complex was assessed using standard methods [17] against numerous bacterial strains. The antimicrobial inhibition percentage (% A.I.) was evaluated using equation (1).

$$A.I\% = \frac{inhibition\ zone\ diameter\ of\ studied\ compound}{inhibition\ zone\ diameter\ of\ standard} * 100$$

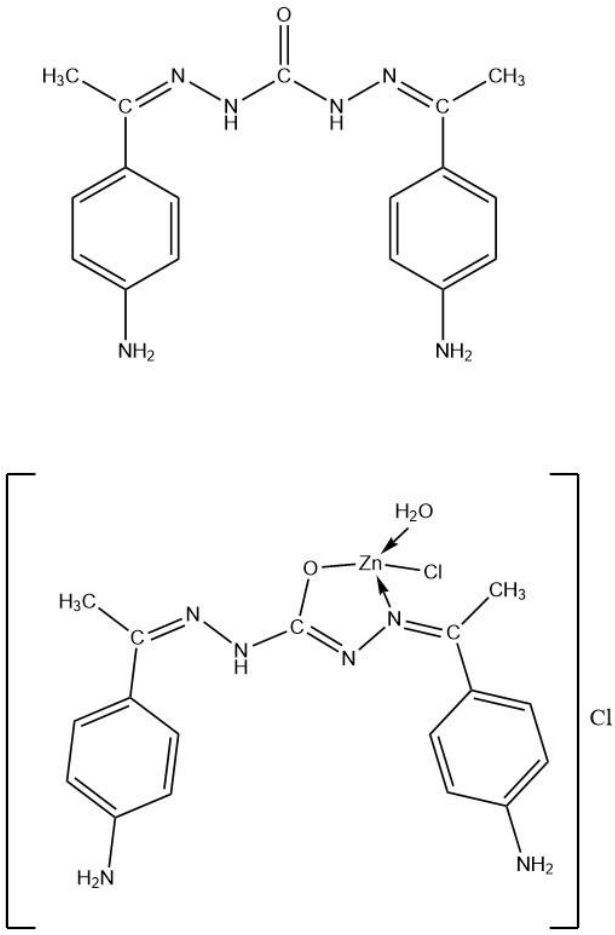

Figure (1): The structures of HL ligand and $[Zn(L)(Cl)(H_2O)].Cl$ complex.

3. Results and discussion

3.1. Molar Conductance Measurements

Adwa Ad 310 conductivity meter was used to assess the electrolytic properties of the isolated Zn(II) complex, the measurement was carried out in 10^{-3}M DMSO solution at room temperature. The results indicated that the Zn(II) complex exhibit a conductance value of 33 (Ω^{-1} cm^2 mol^{-1}) which indicates that the complex have an electrolytic behavior in DMSO solution [18].

3.2. FT-IR Spectroscopy

The FT-IR spectrum of HL ligand and $[Zn(L)(Cl)(H_2O)].Cl$ chelate is illustrated in **Figure 2**. The ligand functions as a monobasic bidentate chelating agent toward Zn(II) ions, as evidenced by the FT-IR spectrum. The disappearance of the carbonyl stretching band and the emergence of a new peak at 1632 cm^{-1} in the Zn(II) complex, attributed to the newly formed (C=N), along with the shift of the original azomethine group to 1595 cm^{-1} and changes in the N-N stretching frequency, confirm the involvement of both the

$\upsilon(C=O)_{carbohydrazone}$ and azomethine $\upsilon(C=N)$ groups in coordination. An absorption band appearing between 3350 and 3500 cm^{-1} suggests the presence of coordinated water in the Zn(II) complex.

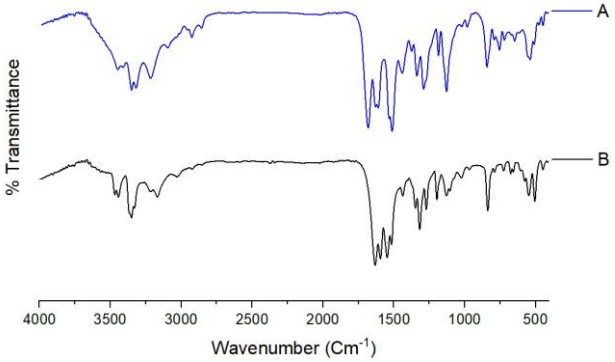

Figure (2): IR spectrum of A. HL ligand and B. Zn(II) complex.

3.3. UV-visible

The electronic spectrum of $[Zn(L)(Cl)(H_2O)].Cl$ complex exhibits most of the characteristic bands of the ligand with slight shifts. These changes in band positions and intensities associated with the complex formation provide evidence of the ligand's coordination to the metal ion.

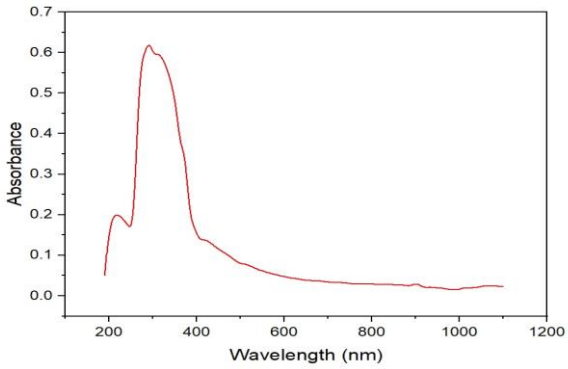

Figure (3): Electronic absorption spectrum of $[Zn(L)(Cl)(H_2O)].Cl$ complex.

3.4. Quantum Computations

3.4.1. Geometry Optimization

The optimized geometry of the isolated Zn(II) complex (Figure 4) was achieved using Material Studio 2017. Ball and stick model was used to visualize the structure and atom numbering of Zn(II) complex. **Table 1** and **Table 2** shows the detailed information about the bond lengths and angles of the bonds which indicated the following information.

A. Firstly, the ligand bond angles were altered slightly after complexation. Also, it was expected that the bonds may be shortened or elongated on coordination as a result of bonding.

B. The formation of M-N and M-O The chelation process, involving the formation of M-N and M-O bonds between the ligand's donor groups and the metal ions, weakens the C=O and C=N bonds. This results in an elongation of the bond lengths in the carbonyl group and the C=N moiety of carbohydrazone.

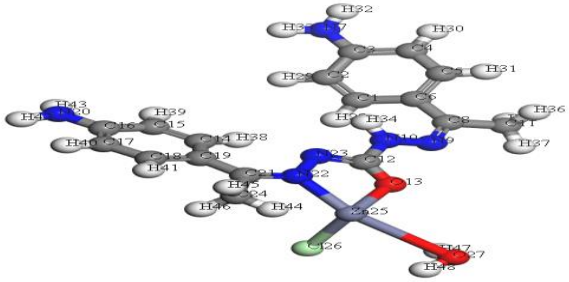

Figure (4): optimized geometry of Zn(II) complex

Table 2. Bond lengths of Zn(II) Complex

Bond	Length	Bond	Length	Bond	Length
O(27)-H(48)	0.985	C(17)-C(18)	1.416	1.510	1.497
O(27)-H(47)	0.985	C(16)-N(20)	1.392	1.362	1.260
O(27)-Zn(25)	3.431	C(16)-C(17)	1.430	1.028	1.050
Cl(26)-Zn(25)	2.591	C(15)-H(39)	1.101	1.028	1.050
C(24)-H(46)	1.110	C(15)-C(16)	1.432	1.469	1.503
C(24)-H(45)	1.113	C(14)-H(38)	1.093	1.098	1.100
C(24)-H(44)	1.108	C(19)-C(14)	1.444	1.442	1.420
N(22)-Zn(25)	2.309	C(14)-C(15)	1.418	1.100	1.100
N(22)-N(23)	1.344	O(13)-Zn(25)	2.218	1.416	1.420
C(21)-C(24)	1.509	N(23)-C(12)	1.378	1.393	1.462
C(21)-N(22)	1.379	C(12)-O(13)	1.294	1.432	1.420
N(20)-H(43)	1.027	C(11)-H(37)	1.106	1.101	1.100
N(20)-H(42)	1.028	C(11)-H(36)	1.114	1.431	1.420
C(19)-C(21)	1.459	C(11)-H(35)	1.110	1.098	1.100
C(18)-H(41)	1.096	N(10)-H(34)	1.035	1.444	1.420
C(18)-C(19)	1.448	N(10)-C(12)	1.402	1.418	1.420
C(17)-H(40)	1.100	N(9)-N(10)	1.359		

Table 3. Bond Angles of Zn(II) Complex

Bond	Angle	Bond	Angle	Bond	Angle
H(48)-O(27)-H(47)	103.103	C(18)-C(19)-C(14)	116.187	H(34)-N(10)-N(9)	121.351
H(48)-O(27)-Zn(25)	78.574	H(41)-C(18)-C(19)	120.124	C(12)-N(10)-N(9)	120.811
H(47)-O(27)-Zn(25)	74.649	H(41)-C(18)-C(17)	117.771	N(10)-N(9)-C(8)	119.565
O(27)-Zn(25)-Cl(26)	74.684	C(19)-C(18)-C(17)	122.103	C(11)-C(8)-N(9)	113.615
O(27)-Zn(25)-N(22)	161.425	H(40)-C(17)-C(18)	119.673	C(11)-C(8)-C(6)	120.380
O(27)-Zn(25)-O(13)	87.920	H(40)-C(17)-C(16)	119.751	N(9)-C(8)-C(6)	126.005
Cl(26)-Zn(25)-N(22)	108.279	C(18)-C(17)-C(16)	120.576	H(33)-N(7)-H(32)	114.858
Cl(26)-Zn(25)-O(13)	104.340	N(20)-C(16)-C(17)	120.620	H(33)-N(7)-C(3)	118.369
N(22)-Zn(25)-O(13)	73.542	N(20)-C(16)-C(15)	120.912	H(32)-N(7)-C(3)	118.336
H(46)-C(24)-H(45)	107.209	C(17)-C(16)-C(15)	118.423	C(8)-C(6)-C(5)	120.291
H(46)-C(24)-H(44)	108.053	H(39)-C(15)-C(16)	119.636	C(8)-C(6)-C(1)	122.678
H(46)-C(24)-C(21)	112.163	H(39)-C(15)-C(14)	119.504	C(5)-C(6)-C(1)	116.944
H(45)-C(24)-H(44)	107.015	C(16)-C(15)-C(14)	120.857	H(31)-C(5)-C(6)	119.875
H(45)-C(24)-C(21)	111.917	H(38)-C(14)-C(19)	119.588	H(31)-C(5)-C(4)	118.584
H(44)-C(24)-C(21)	110.252	H(38)-C(14)-C(15)	118.604	C(6)-C(5)-C(4)	121.517
N(22)-N(23)-C(12)	114.277	C(19)-C(14)-C(15)	121.801	H(30)-C(4)-C(5)	119.714
Zn(25)-N(22)-N(23)	113.396	Zn(25)-O(13)-C(12)	111.957	H(30)-C(4)-C(3)	119.603
Zn(25)-N(22)-C(21)	123.590	N(23)-C(12)-O(13)	126.640	C(5)-C(4)-C(3)	120.682
N(23)-N(22)-C(21)	122.245	N(23)-C(12)-N(10)	112.988	N(7)-C(3)-C(4)	120.638
C(24)-C(21)-N(22)	113.437	O(13)-C(12)-N(10)	120.367	N(7)-C(3)-C(2)	120.598
C(24)-C(21)-C(19)	119.510	H(37)-C(11)-H(36)	107.229	C(4)-C(3)-C(2)	118.708
N(22)-C(21)-C(19)	126.950	H(37)-C(11)-H(35)	109.108	H(29)-C(2)-C(3)	120.039
H(43)-N(20)-H(42)	114.675	H(37)-C(11)-C(8)	109.894	H(29)-C(2)-C(1)	119.468
H(43)-N(20)-C(16)	118.253	H(36)-C(11)-H(35)	106.913	C(3)-C(2)-C(1)	120.483
H(42)-N(20)-C(16)	118.118	H(36)-C(11)-C(8)	111.911	H(28)-C(1)-C(6)	120.069
C(21)-C(19)-C(18)	119.001	H(35)-C(11)-C(8)	111.626	H(28)-C(1)-C(2)	118.080
C(21)-C(19)-C(14)	124.690	H(34)-N(10)-C(12)	117.671	C(6)-C(1)-C(2)	121.621

3.4.2. Frontier Molecular Energies

Frontier molecular orbitals, specifically the HOMO and LUMO, play a key role in determining chemical reactivity. Molecules with smaller HOMO and LUMO gaps exhibit higher reactivity and greater susceptibility to charge transfer due to their lower stability and increased softness. 3D illustration of HOMO and LUMO orbitals of Zn(II) is represented in **Fig. (5)**. The energies of the frontier orbitals, including HOMO and LUMO values, are listed in **Table 3**. These values form the foundation for calculating several key parameters that are also presented.

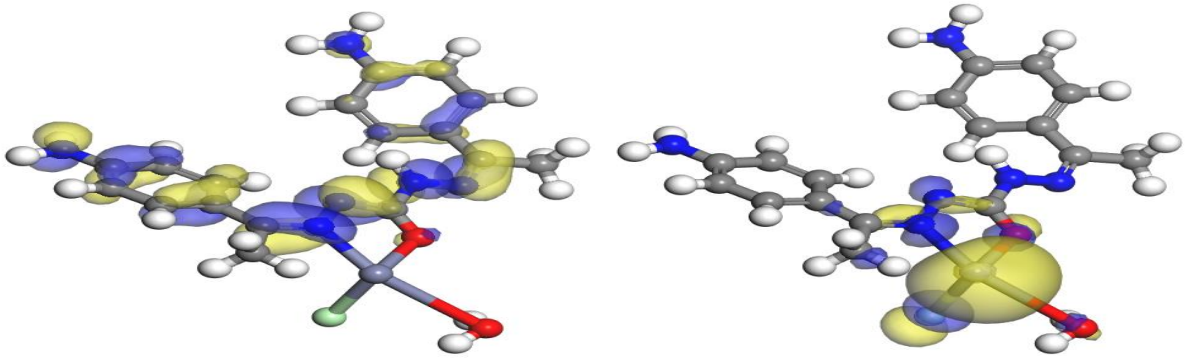

HOMO **LUMO**

Figure (5): HOMO and LUMO orbitals of Zn(II) complex

Table 4. Computed Values of Zn(II) complex

Compound	E_H(eV)	E_L(eV)	(E_H-E_L) (eV)	χ(eV)	μ(eV)	η(eV)	S(eV^{-1})	ω(eV)
Zn(II) Complex	-4.380	-3.028	-1.352	3.704	-3.704	0.676	0.338	10.147

3.4.3. Molecular Electrostatic Potential Maps (MESP)

The Molecular Electrostatic Potential (MESP) is a 3D representation of the energy potential generated by a molecule's electron distribution. It provides insights into charge distribution and aids in predicting chemical reactivity. By analyzing a molecule's electrostatics, one can understand its interactions with the surrounding environment. MESP is particularly valuable in the study of biomolecules, such as DNA and proteins, and plays a crucial role in drug and material design (Figure 6).

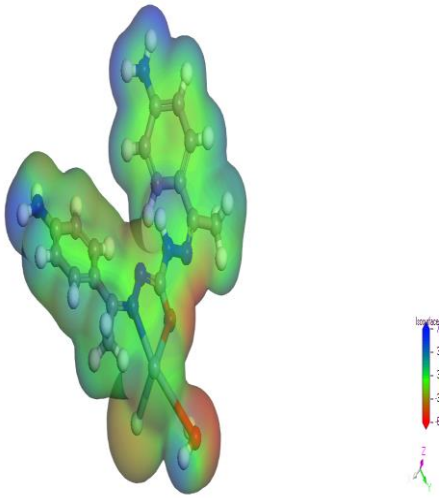

Figure 6: Colored MESP Map of Zn(II) Complex

3.6. Biological efficacy.

3.6.1. Antimicrobial Studies

The *in vitro* antimicrobial activity of the [Zn(L)(Cl)(H2O)].Cl complex was evaluated against a range of bacterial strains, including two Gram positive bacteria, (*Staphylococcus aureus* and *Listeria*), as well as two Gram negative bacteria, (*Klebsiella pneumoniae* and *Salmonella*).

Ampicillin was used as a reference standard to evaluate antibacterial activity. Additionally, antifungal activity was tested against Aspergillus, with Clotrimazole serving as the reference standard, as outlined in **Table 4**. The following findings were derived from the experimental evaluation of antimicrobial activities:

1. The coordination compound [Zn(L)(Cl)(H_2O)].Cl exhibited an absence of antimicrobial efficacy against *Listeria*.

2. In contrast, the complex exhibited markedly higher antibacterial activity against *K. pneumoniae* compared to the other bacterial strains.

3. The complex demonstrated negligible activity against the *Aspergillus* fungal strain.

Table (5): The measurement of bacterial sensitivity (mm) exhibited by the [Zn(Cl)(H_2O)].Cl complex in relation to various bacterial and fungal strains.

	S.aureus		*Listeria*		*K.pneumoniae*		*salmonella*		*Aspergillus*	
	D (mm)	% A.I	D(mm)	% A.I	D (mm)	%A.I	D (mm)	% A.I	D (mm)	% A.I
Ampicillin	23	100	25	100	24	100	22	100	--	--
Clotrimazole	--	--	--	--	--	--	--	--	29	100
[Zn(L)(Cl)(H_2O)].Cl	5	20	--	--	10	40	11	50	--	--

Conclusion

In this study, a novel Zn(II) complex was successfully synthesized from the carbohydrazone Schiff base ligand. The results revealed that the newly synthesized complex displayed a tetrahedral arrangement around the Zn(II) ion. Additionally, the infrared spectrak data indicated that the ligand acted as a bidentate (NO) ligand, coordinating with the metal center. The conductance measurements indicated that the complex exhibits an electrolytic nature in DMSO solution. The results were confirmed through computational

studies which confirmed the proposed geometry of the isolated complex. Additionally, computed values such as band gap, chemical potential, electronegativity, global hardness, global softness measure of polarizability, and global electrophilicity index were calculated. Finally, the antimicrobial activity of the isolated complex was assessed.

References

.1 Alka, et al., (2023) Pharmacological aspects of Co(II), Ni(II) and Cu(II) schiff base complexes: An insight. Results in Chemistry,. **5**: p. 100849.

.2 Abu-Dief, A.M. and I.M.A. Mohamed, A (2015) review on versatile applications of transition metal complexes incorporating Schiff bases. Beni-Suef University Journal of Basic and Applied Sciences,. **4**(**2**): p. 119-133.

.3 Michael, S., et al., (2023) Influence of electron density on the biological activity of aniline substituted Schiff base: in silico, in vivo and in vitro authentication. *Journal of Molecular Structure*,. **1279**: p. 134987.

.4 Uddin, N., et al., (2020) Synthesis, characterization, and anticancer activity of Schiff bases. *Journal of Biomolecular Structure and Dynamics*,. **38**(11): p. 3246-3259.

.5 Malik, M.A ،.et al., (2018) Heterocyclic Schiff base transition metal complexes in antimicrobial and anticancer chemotherapy. MedChemComm,. **9**(**3**): p. 409-436.

.6 Almehmadi, S.J., et al., (2022) Solvent free synthesis, characterization, DFT, cyclic voltammetry and biological assay of Cu(II), Hg(II) and UO2(II) – Schiff base complexes. *Arabian Journal of Chemistry*,. **15**(2): p. 103586.

.7 Singh, R.B., P. Jain, and R.P. Singh, (1982) Hydrazones as analytical reagents: a review. Talanta,. **29**(2): p. 77-84.

.8 Halli, M.B., R.B. Sumathi, and M. Kinni, (2012) Synthesis, spectroscopic characterization and biological evaluation studies of Schiff's base derived from naphthofuran-2-carbohydrazide with 8-formyl-7-hydroxy-4-methyl coumarin and its metal complexes. Spectrochimica Acta Part A: Molecular and Biomolecular Spectroscopy,. **99**: p. 46-56.

.9 Halli, M.B. and R.B. Sumathi, (2012) Synthesis, spectroscopic, antimicrobial and DNA cleavage studies of new Co(II), Ni(II), Cu(II), Cd(II), Zn(II) and Hg(II) complexes with naphthofuran-2-carbohydrazide Schiff base. *Journal of Molecular Structure*,. **1022**: p. 130-138.

.10 Halli, M.B. and R.B. Sumathi, (2014) Antimicrobial, DNA cleavage, and antioxidant properties of new series of metal(II) complexes derived from naphthofuran-2-carbohydrazide Schiff base: synthesis and physico-chemical studies. Medicinal Chemistry Research,. **23**(**4**): p. 2093-2105.

.11 Alharbi, A., et al., (2022) Green synthesis approach for new Schiff's-base complexes; theoretical and spectral based characterization with in-vitro and in-silico screening. *Journal of Molecular Liquids*,. **345**: p. 117803.

.12 Majeed, N.S., H.F. Mohsen, and R.A.B. Aldujaili, (2018) Synthesis, characterization and biological activity of some new heterocyclic compounds derived from 4-aminoacetophenone. Biochem. Cell. Arch,. **18**(1): p. 1107-1116.

.13 Al-qatrani, N.H.K., A.H. Essa, and S.A. Al-Jadaan. (2019) Synthesis, Characterization and Antibacterial Activity of Some New 1, 2, 3-Selenadiazole derived from 4-amino acetophenone. in *Journal of Physics: Conference Series*. .IOP Publishing.

.14 Raouf, O.H., et al., (2020) Synthesis, characterization and biological activity of Schiff bases based on chitosan and acetophenone derivatives. AJCA,. **3**: p. 274-282.

.15 Jeffery, G., (2022) Vogel's Textbook of Quantitative Chemical Analysis 5th Ed.: A John Wiley & Sons, INC.

.16 El-Helw, Mohab A., et al., (2024) Synthesis, Characterization, Biological Potency, and Molecular Docking of Co2+, Ni2+, and Pd2+ Complexes Derived From Carbohydrazone Ligand and Its Application in Dye Removal. Applied

Organometallic Chemistry,. **n/a**(n/a): p. e7830.

.17 Zaky, R.R., T.A. Yousef, and K.M. Ibrahim, (2012*)* Co(II), Cd(II), Hg(II) and U(VI)O2 complexes of o-hydroxyacetophenone[N-(3-hydroxy-2-naphthoyl)] hydrazone: Physicochemical study, thermal studies and antimicrobial activity. Spectrochimica Acta Part A: Molecular and Biomolecular Spectroscopy,. **97**: p. 683-694.

.18 Geary, W.J., (1971) The use of conductivity measurements in organic solvents for the characterisation of coordination compounds. Coordination Chemistry Reviews,. **7**(**1**): p. 81-122.